Journal of Oceanography, Vol. 64, pp. 631 to 637, 2008

Ocean-Atmosphere Momentum Coupling in the Kuroshio Extension Observed from Space

W. Timothy Liu* and Xiaosu Xie

Jet Propulsion Laboratory, California Institute of Technology, Pasadena, CA 91109, U.S.A.

(Received 1 December 2007; in revised form 3 March 2008; accepted 11 March 2008)

Using a combination of Quick Scatterometer (QuikSCAT), Advanced Microwave Scanning Radiometer-Earth Observing System (AMSR-E), and Lagrangian drifter measurements, we demonstrate that wind data alone are not sufficient to derive ocean surface stress (momentum flux) over mid-latitude ocean fronts, specifically the Kuroshio Extension. There was no continuous and large-scale stress measurement over ocean until the launch of the scatterometers. Stress had been derived from winds through a drag coefficient, and our concept of stress distribution may be largely influenced by our knowledge of wind distribution. QuikSCAT reveals that the variability of stress could be very different from wind. The spatial coherence between the magnitude of stress and sea surface temperature (SST), between the divergence of surface stress and the downwind SST gradient, and between the vorticity of stress and crosswind SST gradient, are the inherent characteristics of stress (turbulence production by buoyancy) that would exist even under a uniform wind field. The coherence between stress vorticity and SST gradient is masked by the rotation of ocean currents over the Kuroshio meanders. Surface stress rotates in the opposite direction to surface currents because stress is the vector difference between wind and current. The results are in agreement with a previous study of the Agulhas Extension and confirm the unique stress measuring capability of the scatterometer.

Keywords:
· Wind-stress,
· ocean-front,
· buoyancy,
· current-shear,
· scatterometer,
· ocean-atmosphere-coupling,
· divergence,
· vorticity.

1. Introduction

Ocean surface stress (τ) is the momentum flux that drives ocean circulation. The two-dimensional τ field is needed to compute the divergence and curl (vorticity) that control the vertical mixing. The mixing brings short-term momentum and heat trapped in the surface mixed layer into the deep ocean, where they are stored over time, and brings nutrients and carbon stored in the deep ocean to the surface, where there is sufficient light for photosynthesis. The horizontal currents, driven in part by τ, distribute the stored heat and carbon in the ocean. Until the launch of the scatterometer, our knowledge of τ distribution was largely derived from winds measured at ships and buoys, or from the operational wind product of numerical weather prediction (NWP) centers, through a drag coefficient.

Traditional methods of parameterization of stress and their assumptions are discussed in Section 2. The unique capability of the space-based scatterometer in measuring stress rather than wind vector is demonstrated over the current and temperature fronts of the Kuroshio Extension in the northern Pacific Ocean, following the study of Liu *et al*. (2007) of the Agulhas Extension in the Southern Indian Ocean. The present inadequacy of the parameterization of τ in terms of wind and the significance of stress measurement by the scatterometer is examined.

2. Relation between Wind and Stress

Stress is the turbulent transfer of momentum, and turbulence is generated by atmospheric instability caused both by wind shear (difference between wind and current) and buoyancy (vertical density stratification resulting from temperature and humidity gradients). Direct τ measurement has only been done in a few field campaigns in the past (e.g., Smith, 1980). For all practical purposes, our knowledge of τ is derived from winds (u) through turbulence parameterization. The relation between τ and u at a height z, in terms of an empirical drag coefficient (C_D), has been studied extensively and is governed by the flux-profile relation (e.g., Liu *et al*., 1979):

* Corresponding author. E-mail: W.Timothy.Liu@jpl.nasa.gov

$$\frac{u-u_s}{u_*} = 2.5\left(\ln\frac{z}{z_0} - \psi\right) = \frac{1}{\sqrt{C_D}}, \qquad (1)$$

where u_s is the surface current, $u_* = (\tau/\rho)^{1/2}$ is the frictional velocity, ρ is the air density, z_0 is the roughness length, and ψ is a function of the stability parameter, which is the ratio of buoyancy to shear production of turbulence. The effects of sea state and surface waves (e.g., Donelan *et al*., 1997) are not included explicitly in the relation. In general oceanographic applications the surface current is assumed to be small compared with wind and the atmosphere is assumed to be nearly neutral. Neglecting u_s and ψ, C_D is a constant or a function of wind speed alone.

Advection, rolls (secondary flow), organized convection, and similar circulation factors affect boundary-layer dynamics and winds, but their effects on τ have to be manifested through surface turbulence according to Eq. (1) (e.g., Brown and Liu, 1982). Near the surface, flux divergence, baroclinicity, and Coriolis force can be neglected.

3. Data Processing

The principle of scatterometry and the history of scatterometer missions have been reviewed by Liu (2002). The scatterometer sends microwave pulses to the Earth's surface and measures the backscatter power. Over the ocean, the backscatter power is largely caused by small, centimeter-scale waves on the surface, which are believed to be in equilibrium with τ. Liu and Large (1981) demonstrated, for the first time, the relation between measurements by a space-based scatterometer and surface stress measured on research ships. There are much less stress than wind measurements for validation and calibration of the scatterometer. The geophysical data product of the scatterometer is the equivalent neutral wind (ENW) at 10 m height (Liu and Tang, 1996), which, by definition, is uniquely related to τ, while the relation between τ and the actual winds at the reference level depends on atmospheric stability and the ocean's surface current.

ENW, similar to the frictional velocity, can be viewed as stress scaled to the wind unit. Starting with in-situ measurements made under stable and unstable conditions, u_* and z_0 are computed (as the gradient and intercept at the surface) as defined in Eq. (1), the flux-profiles relation of Liu *et al*. (1979). With u_* and z_0, ENW is computed neglecting ψ. As discussed by Liu and Tang (1996) and shown in Liu *et al*. (2007), ENW is higher than u under unstable conditions and lower than u under stable conditions. The computed ENW, of course, depends on ψ, which represents the state-of-the-art of turbulence parameterization (Liu *et al*., 1979). Although there have been many investigations into improving the drag coefficient (e.g., Fairall *et al*., 1996) in the past few decades, no significant changes have been introduced in the formulation. ENW at 25 km resolution starting from June 2002 is used in this study.

AMSR-E, on board NASA's Aqua satellite, was launched in May 2002 and has been collecting global SST under clear and cloudy conditions. SST, averaged to 0.25° by 0.25° grids for ascending and descending paths (Wentz and Meissner, 1999), was obtained from the Remote Sensing System and monthly averages were calculated.

Recently, more than a decade-long series of a global data set of near surface current has been made available. The current velocity was derived from Argos satellite collections of the displacements of drifters with drogues centered at 15m-depth (Niiler, 2001). Five years of data from January 2000 to December 2004 were averaged and used in this study.

The altimeter products were produced by SSALTO (Segment Sol multimissions d'ALTimétrie, d'Orbitographie et de localisation precise)/DUACS (Data Unification and Altimeter Combination System) and distributed by AVISO (Archiving, Validation and Interpretation of Satellite Oceanographic data), with support from CNES (Centre National d'Études Spatiale). The merged data sets combine all available satellites with inter-calibration (Ducet *et al*., 2000) including TOPEX/Poseidon, Jason-1, ERS-1/2, Geosat Follow-On (GFO), and Envisat, with 0.25° × 0.25° and weekly resolution.

The operational NWP analysis products of the National Center for Environmental Prediction (NCEP) at 1° resolution were obtained from the National Center for Atmospheric Research. The high-resolution surface wind vectors (at 1°) of the European Center for Medium Range Weather Forecast (ECMWF) were obtained for the same periods by the QuikSCAT projects for validation purposes under special arrangements.

To separate the features related to the Kuroshio Extension meanders from the large-scale spatial gradients, a two-dimensional filter was applied to the monthly mean of all parameters. The filter essentially removes the running mean with scales of 10° in longitude and 2° in latitude, weighted by a sine function. The deviations from the running mean were averaged through the available data period to construct the long-term mean anomalies; they are referred to as anomalies hereafter. The circular anomaly features associated with the Kuroshio Extension meanders are referred to as eddies. For the zonal (U) and meridional (V) components of a vector (ENW or surface current), the convergence ($-\partial U/\partial x - \partial V/\partial y$) and vorticity ($\partial V/\partial x - \partial U/\partial y$) anomalies are computed from the long-term means of U and V anomalies. Vorticity is the vertical component of the curl of the vector.

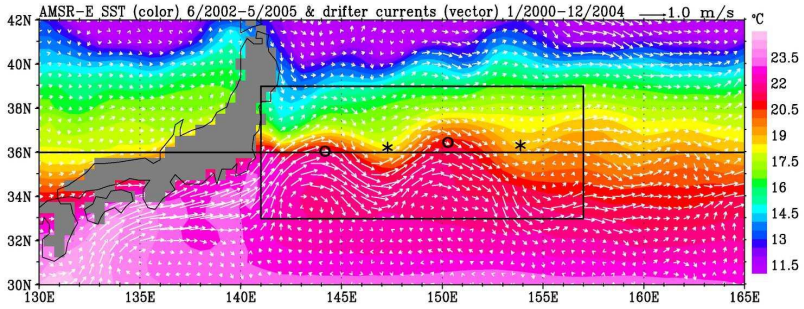

Fig. 1. Ocean surface current measured by Lagrangian drifters (white arrows) superimposed on SST (color, °C) from AMSR-E. Circles and stars represent centers of warm and cold SST anomalies.

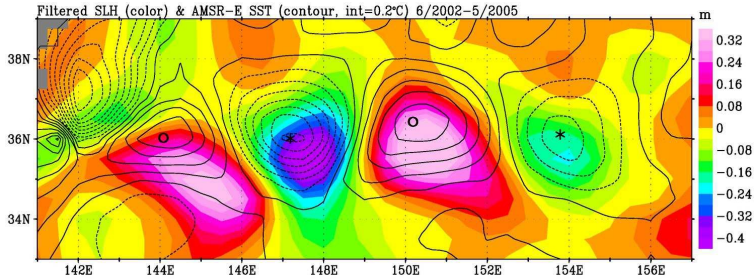

Fig. 2. Isotherms of filtered SST measured by AMSR-E (0.2°C interval) superimposed on filtered sea level variation from merged altimeter data (color, m). Solid and broken lines represent positive and negative values, respectively.

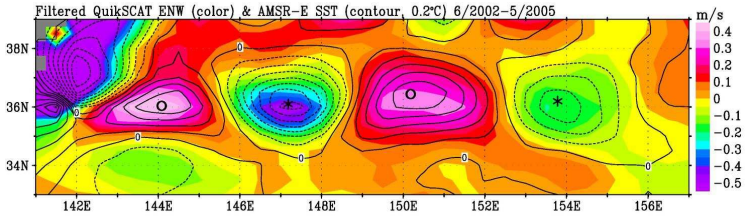

Fig. 3. As Fig. 2, except that QuikSCAT ENW replaces sea level variation.

4. Analysis

The drifter data reveal that the Kuroshio Current separates from the coast of Japan at about 36°N to form the Kuroshio Extension across the Pacific (Fig. 1). Two quasi-permanent meanders, with ridges at 144°E and 150°E, are examined in this study. The existence of these meanders has been discussed in a number of studies (e.g., Qiu, 2002; Niiler *et al*., 2003). A cyclonic current causes divergence and upwelling of cold water, while an anti-cyclonic current causes downwelling. Cold SST, as measured by AMSR-E, is located with the cyclonic current; warm SST is located with anticyclonic currents, as shown in the figure. Although SST data are averaged only over a three-year period (June 2002 to May 2005) and surface currents are averaged over a five-year period (January 2000 to December 2004), the centers of their anomalies are approximately collocated. Drifter data are sparse and it takes five years to cover the region adequately.

The SST anomalies caused by the current meander within the region marked by the rectangular box in Fig. 1 are more clearly exhibited by the isotherms in Fig. 2, after the filtering described in Section 3. The centers of sea level anomalies measured by radar altimeters, which reflects the dynamic and steric changes over the whole water column, are displaced only slightly to the south-east of the SST anomalies (Fig. 2), which confirms the

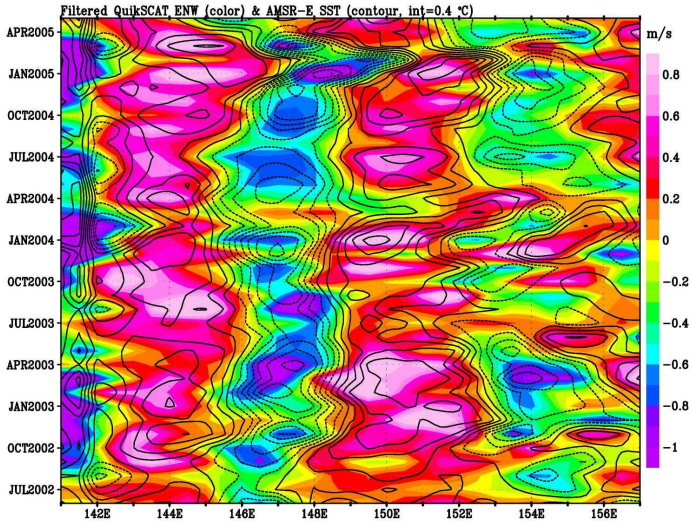

Fig. 4. Time-longitude variations of filtered magnitude of ENW (color, m/s) and SST (isotherm, 0.4°C interval) at 36°N.

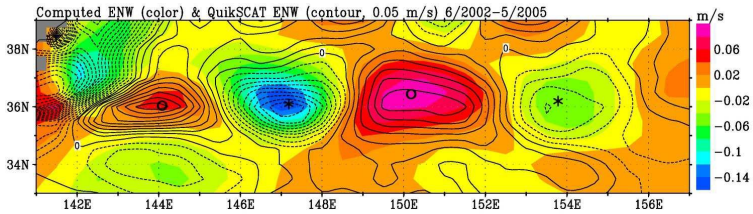

Fig. 5. Contour of filtered magnitude of QuikSCAT ENW (0.05 m/s interval) superimposed on filtered magnitude of ENW computed from a uniform wind field (color, m/s).

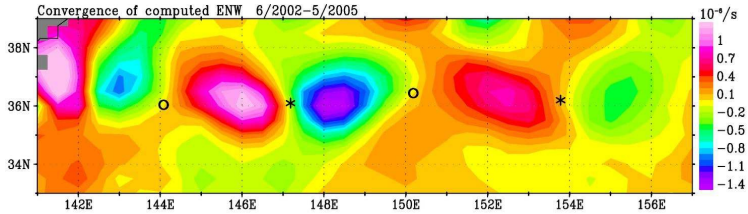

Fig. 6. Convergence of filtered ENW computed from a uniform wind field (unit is 10^{-6}/s).

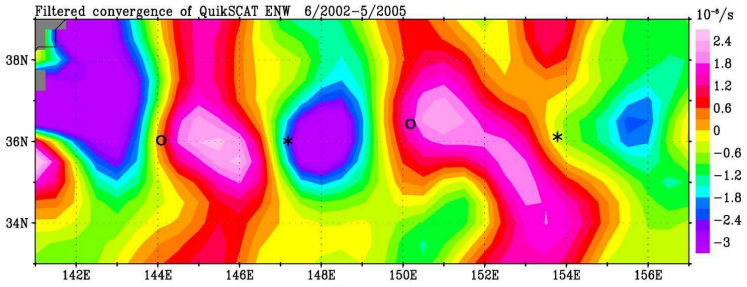

Fig. 7. Convergence of filtered ENW observed by QuikSCAT (unit is 10^{-6}/s).

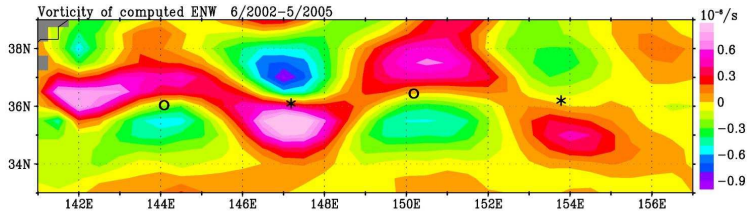

Fig. 8. Vorticity of filtered ENW computed from a uniform wind field (unit is 10^{-6}/s).

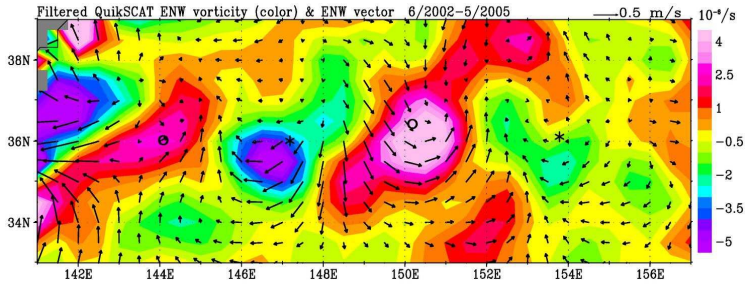

Fig. 9. Filtered vector (black arrows) superimposed on vorticity (color, 10^{-6}/s) of ENW observed by QuikSCAT.

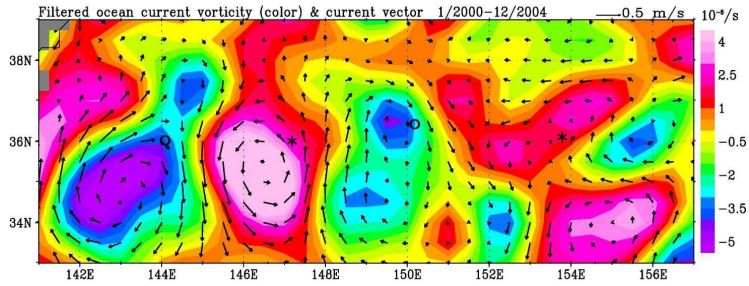

Fig. 10. Filtered vector (black arrows) superimposed on vorticity (color, 10^{-6}/s) of the surface current measured by Lagrangian drifters.

ocean upwelling associated with the meanders.

The collocation of and the positive correlation between the magnitude of ENW (or τ) measured by QuikSCAT and SST are clearly demonstrated in Fig. 3. Positive ENW anomalies are found over warmer water and negative anomalies over cooler water. The quasi-stationary nature of these two meanders is demonstrated in Fig. 4. High SST and ENW persist at 144°E and 150°E, while low SST and ENW persist at 146.5°E and 154°E, with exceptions in a few months (e.g., November 2003 and February 2005). The stationary nature is weaker at the eastern end of the meander centered at 154°E.

To illustrate that the coherence between QuikSCAT measurements and SST is inherent in the definition of ENW (turbulent mixing theory), a conceptual experiment is performed. A uniform wind field at 10 m height is assumed, with speed of 7.1 m/s blowing from west to east, which is the average of ECMWF winds for the region for the three-year period. Using AMSR-E SST and NCEP air temperature and humidity at each grid location with this constant wind field, ENW is computed with the method described in Section 2. Figure 5 shows that the anomalies of computed ENW magnitude have a coherence with SST that is similar to the QuikSCAT measurements shown in Fig. 3, although the spatial variation of the computed ENW is weaker than the observed variation. In reality, the wind field should not be uniform but adjusts to surface stress changes. The temperature and humidity from NCEP do not accurately simulate the small-scale variation over the ocean meanders.

Figure 6 shows that the convergence of the computed ENW is in quadrature (90° phase difference) with SST in the downwind direction. This correlation implies that the convergence is in-phase with the downwind SST gradient. A similar quadrature spatial correlation is observed between SST and QuikSCAT ENW, as shown in Fig. 7. The convergence on the downwind side of the high SST anomalies is the result of deceleration of ENW. The convergence and divergence may result in ascending and descending air motion, respectively. The convective cell may increase ENW over warm water and decrease ENW over cold water; it may provide a positive feedback to the ENW-SST coherence resulting from stability difference.

Figure 8 shows that the vorticity of the computed ENW is in quadrature with SST in the crosswind direction; vorticity is in-phase with the crosswind SST gradient. Positive vorticity is found to the south and negative anomalies to the north of the cold eddy, and vice versa for the warm eddy. QuikSCAT observations, however, do not show such crosswind relation (Fig. 9). Positive observed vorticity is collocated (in-phase) with warm water and negative vorticity is collocated with cold water. The vorticity of the observed ENW is opposite to the vorticity of the surface current measured by drifters (Fig. 10). Stress depends on the vector difference between wind and current. With non-rotating winds overhead, stress should rotate in the opposite direction to the current, as postulated by Park *et al*. (2006), with reference to the Gulf Stream rings.

The opposite sign of the vorticity implies that the stress spins down the current rotation. The ENW vorticity, however, is smaller than current vorticity. The current shear at the meanders is maintained by the energy brought in by the Kuroshio and is not driven by surface winds. Although the drifters measure current at 15 m depth, the vorticity of the current should dominate over current vorticity at the surface. The current divergence is small and ENW divergence is largely caused by SST gradient, unaffected by surface current.

5. Discussion

This study of the Kuroshio Extension in the North Pacific Ocean supports and extends the findings of Liu *et al*. (2007) on the Agulhas Extension in the Southern Indian Ocean. The results confirm that the scatterometer measures stress and not wind, and the variation of stress could be very different from that of wind.

The strong ocean current should impart its rotation on the prevailing westerly wind through drag. If the scatterometer measures wind, we would expect the measurement (ENW) to show the same rotation as the current. QuikSCAT measurements in opposition to the rotation of surface current, however, have been observed in Gulf Stream rings (e.g., Park *et al*., 2006), in the Agulhas Extension (Liu *et al*., 2007) and over the Kuroshio as in this study. The rotation of ENW is a clear characteristic of stress, the turbulence produced by the shear between wind and current vectors.

The coherence between the ENW convergence and downwind SST gradient and between the ENW vorticity and crosswind SST gradients, as also described by previous investigations (e.g., O'Neill *et al*., 2005), is a direct consequence of the unique stress measuring capability of the scatterometer and the dependence on turbulence production by buoyancy. The spatial coherence between the magnitude of ENW measured by QuikSCAT and SST has been extensively observed (e.g., Xie *et al*., 1998, 2002; Liu *et al*., 2000; Wentz *et al*., 2000; Chelton *et al*., 2001; Lin *et al*., 2003). Such coherence is ubiquitous and very clear when the mean gradients are filtered out, as shown in this study. It is also evident without filtering, as shown in the frequency of high ENW (Sampe and Xie, 2007) and in the probability distribution function of the full spectrum of ENW magnitude (Liu *et al*., 2008). The changes of ENW are so well collocated with SST under a broad range of atmospheric circulations because, at the small turbulence (stress) scales, the factors that govern boundary layer and larger-scale dynamics, such as flux divergence, baroclinicity, and Coriolis force, are not important. Larger-scale atmospheric circulation may be modified by but is not the main driving force of the spatial coherence, which disagrees with what some of the previous studies tend to imply.

Although the scatterometer has been known to measure surface roughness, which has a closer relation to stress than wind, even before the first demonstration by Liu and Large (1981), it has also been promoted as a wind-measuring instrument. ENW has been used as the actual wind, particularly in operational weather applications. The difference between the variability of stress and wind is assumed to be negligible because the marine atmosphere has near-neural stratification, and the magnitude of ocean current is small relative to wind speed. We are not sure about the extent to which the wind field adjusts to the distribution of ENW (stress) nor whether a bulk parameterization model that includes stability effects (e.g., Liu *et al*., 1979) is sufficient to link the scatterometer observation to wind in different spatial and temporal scales. The present knowledge of the relation between wind and stress may be deficient under the non-stationary and non-homogeneous conditions of ocean fronts and when flow separation occurs in strong winds (as in hurricanes).

The mechanism by which the meso-scale and slow processes of the ocean are propagated upward through stress to affect the fast, large-scale processes of the atmosphere is not sufficiently known. A scenario of posi-

tive atmospheric feedback to the SST-ENW relation through convection that will strengthen the spatial coherence is postulated in Section 4. However, the vertical velocity of convection is not observed. Present numerical models of atmosphere circulation in the mid-latitudes do not propagate ocean SST signals vertically much beyond the atmospheric boundary layer. The lapse rate is believed to be too weak to support deep convection. The observations of SST signatures in cloud and in atmospheric temperature high in the atmosphere by Liu *et al*. (2007) present a challenge to understanding the transition from random turbulence to organized convection, and to improve the dynamic and the spatial versus temporal scale parameterization in a numerical model.

Acknowledgements

This study was conducted at the Jet Propulsion Laboratory, California Institute of Technology, under contract of the National Aeronautics and Space Administration (NASA). It was jointly supported by the Physical Oceanography and Ocean Vector Wind Programs of NASA. Sharon Schneider and Pearn P. Niiler kindly provided and advised on the drifter data.

References

Brown, R. A. and W. T. Liu (1982): An operational large-scale marine planetary boundary layer model. *J. Appl. Meteor.*, **2**, 261–269.

Chelton, D. B., S. K. Esbensen, M. G. Schlax, N. Thum, M. H. Freilich, F. J. Wentz, C. L. Gentemann, M. J. McPhaden and P. S. Schoff (2001): Observations of coupling between surface wind stress and sea surface temperature in the eastern tropical Pacific. *J. Climate*, **14**, 1479–1498.

Donelan, M. A., W. M. Drennan and K. B. Katsaros (1997): The air-sea momentum flux in conditions of wind sea and swell. *J. Phys. Oceanogr.*, **27**, 2087–2099.

Ducet, N., P.-Y. Le Traon and G. Reverdin (2000): Global high resolution mapping of ocean circulation from TOPEX/Poseidon and ERS-1 and -2. *J. Geophys. Res.*, **105**, 19477–19498.

Fairall, C. W., E. F. Bradley, D. P. Rogers, J. B. Edson and G. S. Young (1996): Bulk parameterization of air-sea fluxes for Tropical Ocean-Global Atmosphere/Coupled Ocean-Atmosphere Response Experiment (TOGA/COARE). *J. Geophys. Res.*, **101**, 3747–3764.

Lin, I.-I., W. T. Liu, C.-C. Wu, J. C. Chiang and C.-H. Sui (2003): Satellite observations of modulation of surface winds by typhoon-induced upper ocean cooling. *Geophys. Res. Lett.*, **30**(3), 1131, doi:10.1029/2002GL015674.

Liu, W. T. (2002): Progress in scatterometer application. *J. Oceanogr.*, **58**, 121–136.

Liu, W. T. and W. G. Large (1981): Determination of surface stress by Seasat-SASS: A case study with JASIN Data. *J. Phys. Oceanogr.*, **11**, 1603–1611.

Liu, W. T. and W. Tang (1996): Equivalent Neutral Wind. JPL Pub., 96-17, Jet Propulsion Lab., Pasadena, 8 pp.

Liu, W. T., K. B. Katsaros and J. A. Businger (1979): Bulk parameterization of air-sea exchanges in heat and water vapor including the molecular constraints at the interface. *J. Atmos. Sci.*, **36**, 1722–1735.

Liu, W. T., X. Xie, P. S. Polito, S. Xie and H. Hashizume (2000): Atmosphere manifestation of tropical instability waves observed by QuikSCAT and Tropical Rain Measuring Missions. *Geophys. Res. Lett.*, **27**, 2545–2548.

Liu, W. T., X. Xie and P. P. Niiler (2007): Ocean-atmosphere interaction over Agulhas Extension Meanders. *J. Climate*, **20**(23), 5784–5797.

Liu, W. T., W. Tang and X. Xie (2008): Wind power distribution over global oceans. *Geophys. Res. Lett.* (submitted).

Niiler, P. P. (2001): The world ocean surface circulation. p. 193–204. In *Ocean Circulation and Climate—Observing and Modeling the Global Ocean*, ed. by G. Siedler, J. Church and J. Gould, Academic Press, Volume **77** of *International Geophysics Series*.

Niiler, P. P., N. A. Maximenko, G. G. Panteleev, Y. Yamagata and D. B. Olson (2003): Near-surface dynamical structure of the Kuroshio Extension. *J. Geophys. Res.*, **108**(C6), 3193, doi:10.1029/2002JC001461.

O'Neill, L. W., D. B. Chelton, S. K. Esbensen and F. J. Wentz (2005): High-resolution satellite measurements of the atmospheric boundary layer response to SST variation along the Agulhas Return Current. *J. Climate*, **18**, 2706–2723.

Park, K.-A., P. Cornillon and D. L. Codiga (2006): Modification of surface winds near ocean fronts: effects of the Gulf Stream rings on scatterometer (QuikSCAT, NSCAT) wind observations. *J. Geophys. Res.*, **111**, C03021, doi:10.1029/2005JC003016.

Qiu, B. (2002): The Kuroshio Extension System: its large-scale variability and role in the midlatitude ocean-atmosphere interaction. *J. Oceanogr.*, **58**, 57–75.

Sampe, T. and S.-P. Xie (2007): Mapping high sea winds from space. *Bull. Amer. Meteor. Soc.*, **88**, 1965–1978.

Smith, S. D. (1980): Wind stress and heat flux over the ocean in gale force winds. *J. Phys. Oceanogr.*, **10**, 709–726.

Wentz, F. J. and T. Meissner (1999): AMSR Ocean Algorithm, Version 2. RSS Tech. Report 121599A, Remote Sensing Systems.

Wentz, F. J., C. L. Gentemann, D. Smith and D. Chelton (2000): Satellite measurements of sea surface temperature through clouds. *Science*, **288**, 847–850.

Xie, S.-P., M. Ishiwatari, H. Hashizume and K. Takeuchi (1998): Coupled ocean-atmosphere waves on the equatorial front. *Geophys. Res. Lett.*, **25**, 3863–3866.

Xie, S.-P., J. Hafner, Y. Tanimoto, W. T. Liu, H. Tokinaga and H. Xu (2002): Bathymetric effect on the winter climate through the sea surface temperature in the Yellow and East China Seas. *Geophys. Res. Lett.*, **29**(24), 2228, doi:10.1029/2002GL015884.